09

Nonlinear optical properties of single-wall carbon nanotubes for photonics applications

© P.N. Vasilevsky,[1,2] M.S. Savelyev,[1,2,3] A.P. Orlov,[2,4] A.Yu. Gerasimenko[1,2,3]

[1]Institute of Biomedical Systems,
National Research University of Electronic Technology, „MIET“,
124498 Moscow, Zelenograd, Russia
[2]Institute of Nanotechnology of Microelectronics of the Russian Academy of Sciences,
119334 Moscow, Russia
[3]Institute for Bionic Technologies and Engineering,
Sechenov First Moscow State Medical University, Sechenov University,
119991 Moscow, Russia
[4]Kotelnikov Institute of Radio Engineering and Electronics, Russian Academy of Sciences,
125009 Moscow, Russia
e-mail: pavelvasilevs@yandex.ru

Received November 8, 2024 Revised November 8, 2024
Accepted November 8, 2024

The paper studies the nonlinear optical properties of liquid dispersed media with single-wall carbon nanotubes, which manifest themselves when exposed to laser radiation with different parameters, such as energy exposure, duration and pulse repetition rate. The structural properties of the materials under study are studied using Raman scattering, spectroscopy and dynamic light scattering. When exposed to single nanosecond pulses, nonlinear limitation of radiation is recorded, which leads to a sharp decrease in transmission and a decrease in the duration of the pulse passed through the medium. When exposed to femtosecond laser pulses with a high repetition rate (80 MHz), modulation of the spatial shape of the beam is observed due to a change in the refractive index of the medium. It is shown that dispersed media in dimethylformamide exhibit a greater nonlinear optical response in comparison with aqueous media. The authors also demonstrated the possibility of using dispersed media with single-wall carbon nanotubes as laser radiation intensity limiters to protect light-sensitive matrices of optical devices, as well as nonlinear optical switches in optical systems for signal control.

Keywords: single-wall carbon nanotubes, dispersed media, laser radiation, optical limiting, optical switches.

DOI: 10.61011/TP.2025.03.60861.407-24

Introduction

The progress in laser technology in recent decades has led to an expansion of the range of application of lasers [1,2]. New photonic devices operating with laser radiation are required for efficient transmission and processing of optical signals [3]. Such devices are badly needed in the field of lidar design [4], optical communication systems [5], laser location systems [6], medical and scientific laser systems [7], etc.

Of particular interest is the fabrication of passive optical elements [8,9]. These elements are, in contrast to active ones (e.g., electro-optical glasses), capable of adjusting the parameters of laser radiation without any external signal [10]. Materials with nonlinear optical properties were proven to be effective in the design of passive photonic devices [11]. Nonlinear optical media alter their parameters, such as absorption [12] or scattering [13] coefficients, refraction index [14], etc., when exposed to an intense incident light flux. A change in parameters of the medium leads to a corresponding change in parameters of laser pulses (energy, width, direction) emerging from this medium [16]. Such fast nonlinear optical effects as inverse saturable absorption or multiphoton absorption allow one to manipulate laser pulses of a nanosecond width, which ensures high speed of operation with optical signals. Nonlinear optical media may serve as the main component of such photonic devices as optical limiters [17], which are needed to protect light-sensitive elements from high-intensity laser radiation, and optical switches, which may be used to transmit logical signals (Fig. 1) [18].

Nonlinear optical media used in photonic devices should offer high transmittance at a low laser power level (in order to minimize the „useful“ optical signal loss) and alter their parameters only upon reaching a certain light intensity, which is called the threshold one [19]. Optical limiter media need to have a broadband response to be able to protect photosensitive arrays within a wide wavelength range [20]. Dispersed media with single-wall carbon nanotubes (SWCNTs) are an example of such materials. In addition to their unique optical properties, SWCNTs are resistant to the effects of high-power laser radiation, providing an opportunity to stabilize the linear optical parameters of the medium [21]. The use of unseparated SWCNTs with mixed chirality provides a broadband response and allows one to achieve a high level of linear transmittance in the visible and near infrared (IR) range by adjusting their concentration [22]. In this case, the

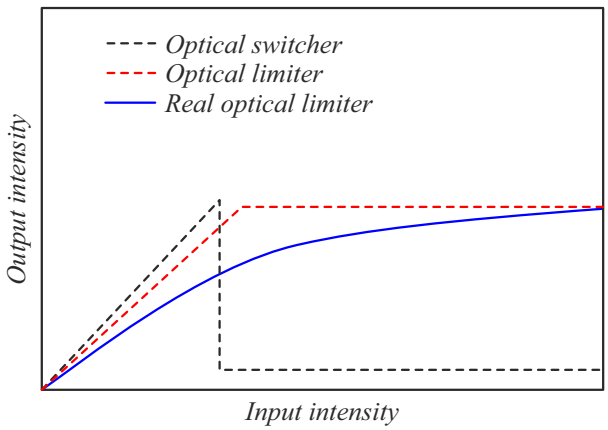

Figure 1. Schematic representation of the operating principle of an optical switch and an optical limiter.

nature of nonlinear interaction depends not only on the nonlinear optical properties of the medium, but also on the type of laser influence, since various nonlinear optical effects may manifest themselves at different pulse width and repetition rate levels. The aim of the present study was to examine the nonlinear optical properties of dispersed media with SWCNTs under the influence of individual nanosecond pulses and femtosecond pulses with a repetition rate of 80 MHz and to assess the feasibility of application of these media in photonics.

1. Materials and research techniques

1.1. Preparation of liquid dispersed media with SWCNTs

SWCNTs of the OSUNT90A type (Uglerod ChG, Russia) in the form of bundles were chosen for studies of nonlinear optical properties. Water and dimethylformamide (DMF) were used as liquid media for dispersion. DMF was chosen for its low absorbance (high transparency) within the wavelength range from the near ultraviolet (UV) to IR. In contrast, water has a strong absorption peak in the ~ 950 nm region. In addition, DMF has a relatively low surface tension (36.42 dyn/cm at room temperature), which increases the dispersibility of heterogeneous systems, including those with carbon nanotubes.

The starting material for preparation of dispersed media based on SWCNTs was an aqueous-based paste with a mass content of SWCNTs of 2.5 %, which was added to the solvent to obtain a concentration of SWCNTs in the dispersion of 0.025 mg/ml. The homogenization procedure was performed after weighing and mixing the components. Since SWCNTs have a large surface area of nanoparticles, this material has a tendency to form large ($\sim 10\,\mu$m) agglomerates. Ultrasonic treatment was performed to break down large agglomerates into small bundles of carbon nanotubes. A Sonicator Q700 (Qsonica, United States) ultrasonic homogenizer operated at a power of 100 W for 1 h was used for this purpose. The temperature during processing did not exceed 45 °C.

An ultrasonic bath and centrifugation were used to remove unmixed large agglomerates of carbon nanotubes from the dispersed medium. Centrifugation was performed for 5 min at a speed of 3500 rpm and a relative centrifugal force of 2260 g. Following this procedure, the upper part of the dispersed medium (supernatant) was separated from the sediment. The supernatant without sediment was used in further studies of nonlinear optical properties. This method of preparation of dispersed media allows one to achieve a homogeneous state, but does not induce untwisting of SWCNT bundles.

1.2. Raman scattering and scanning electron microscopy of SWCNTs

Raman spectra were recorded using an InVia Qontor confocal Raman spectrometer (Renishaw, UK). A laser with a wavelength of 532 nm and a power of 1.09 mW was the excitation source. A diffraction grating with 1200 lines/mm and a 50x visible-range lens were chosen for recording the Raman spectra. A FEI Helios G4 scanning electron microscope (SEM) was used to determine the size of SWCNTs.

1.3. Visible and near IR spectroscopy

A GENESYS 50 UV-Vis spectrophotometer (Thermo Fisher Scientific, United States) was used to evaluate the linear absorption coefficient of dispersed media with SWCNTs. Transmittance T was measured within the wavelength range from 300 to 1100 nm with a pitch of 1 nm. These studies were carried out in a quartz cell with optical path length $d = 3$ mm. Linear absorption coefficient α was determined in the following way:

$$\alpha(\lambda) = -\lg\left(\frac{T(\lambda)}{100\,\%}\right)\Big/ d. \qquad (1)$$

1.4. Dynamic light scattering

Dynamic light scattering (DLS) is a common method for determination of the size distribution profile of nano- and microparticles in a dispersed medium (or polymers in a solution). DLS relies on the Brownian motion of dispersed particles; they move randomly in all directions, losing a part of their energy in collisions. This energy transfer has a more pronounced effect on smaller particles, causing them to move at higher velocities than larger ones. A Photocor Complex particle size analyzer (Photocor, Russia) was used in DLS experiments. It allows one to estimate the size of particles within the range from 0.5 nm to 10 μm.

1.5. Study of nonlinear limiting in dispersed media with SWCNTs

An experimental setup (Fig. 2) for the study of nonlinear limiting in dispersed media with SWCNTs was designed

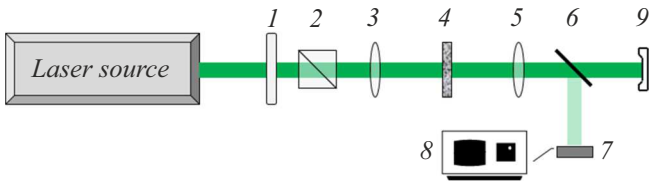

Figure 2. Optical circuit for the examination of nonlinear limiting of laser radiation.

based on an LS-2147N-5 neodymium nanosecond laser (Lotis TII, Belarus). The laser pulse width was 20 ns, and the maximum pulse repetition rate was 10 Hz. The second laser harmonic (532 nm) was used to examine nonlinear optical limiting. A 10CWA168 attenuator (Standa, Lithuania) *1* and a 14GP polarizing Glan–Taylor prism (Standa, Lithuania) *2* were used to adjust the energy of laser radiation affecting the studied sample. Radiation was focused by lens *3*, *5* with a focal length of 10 cm onto the dispersed medium with SWCNTs in a quartz cell with an optical path length of 3 mm. The cell was mounted on a 8MT50-100BS1-MEn motorized translation stage *4* (Standa, Lithuania). Following transmission through the studied sample, a fraction of radiation was directed by means of beam-splitting plate *6* to an OD-08A high-speed photodetector *7* with a photodiode connection (Avesta, Russia), which was used to determine the width of a laser pulse that has passed through the dispersed medium. An MSO64 oscilloscope (Tektronix, United States) *8* was used to estimate the half-width of a pulse. A PD10-C (Ophir, Israel) *9* pyroelectric detector recorded the laser pulse energy.

The *Z*--scanning and fixed sample position techniques were used to study nonlinear limiting of laser radiation under the influence of individual nanosecond pulses. The essence of both techniques lies in varying gradually laser energy fluence F_0 incident on a sample:

$$F_0 = \frac{aU_0}{w_0^2\pi}, \qquad (2)$$

where U_0 is the total energy of the pulse acting on the sample and w_0 is the beam radius. In *Z*-scanning, the energy of radiation incident on the sample remains constant, and the sample is moved along the optical axis on a motorized translation stage. Thus, as the sample approaches the focus of the lens, the beam radius decreases, which leads to an increase in laser energy fluence. The dependence of transmittance (normalized to linear transmittance) on the position of the sample relative to the lens focus is determined in this case. The total energy of radiation affecting the sample was 500 μJ.

In the fixed-position experiment, the sample was mounted at the focus of the lens, and the laser energy fluence was varied by adjusting the energy with an attenuator and a Glan–Taylor polarizing prism. The beam radius at the lens focus was 50 μm. The characteristic dependence for this technique is the dependence of the output energy fluence on the laser energy fluence incident on the sample (limiting curve). The above-described methods and a threshold model based on the radiation transfer equation [23] were used to determine such characteristics of the medium as the effective nonlinear absorption coefficient and the threshold laser energy fluence at which the transition from linear to nonlinear interaction occurs.

1.6. Study of nonlinear refraction in dispersed media with SWCNTs

An experimental setup (Fig. 3) based on a Chameleon Ultra titanium–sapphire femtosecond laser (Coherent, United States) was designed for the study of nonlinear refraction in dispersed media with SWCNTs. The pulse width was 140 fs, the pulse repetition rate was 80 MHz, and the wavelength was 800 nm. Owing to the high pulse repetition rate, the energy of a pulse is very low (on the order of a few nanometers) and does not induce nonlinear absorption. The average radiation power was adjusted by an automatic OAGP-10-S polarizing prism (Avesta, Russia) *1*. Radiation was then focused by a collecting lens onto a quartz cell with a dispersed medium located vertically. Cell *3* was positioned at the focus of lens *2*; the beam radius at the focus was $\sim 90\,\mu$m. The spatial profile of radiation transmitted through the sample and its power were recorded. An SP620U profile analyzer (Ophir, Israel) *4* was used to obtain the spatial radiation profile. The profile analyzer was mounted at a distance of 4 cm from the sample. To record the radiation power affecting the sample, it was removed from the optical axis, and a circular aperture with a diameter of 1 mm was installed instead of the profile analyzer. A 3A power detector (Ophir, Israel) *4* was positioned right behind it. Radiation was transmitted fully through the aperture. When recording the radiation power transmitted through the sample, the aperture was set in such a way that, at low power, radiation did also pass through it unimpaired.

A study of the effect with a horizontal sample arrangement was also carried out. A rectangular prism (Fig. 3, *1.1*), which directed radiation onto the sample, was used in this case. The experimental parameters were similar to those described above.

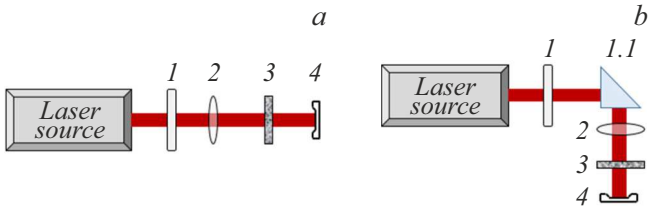

Figure 3. Optical circuit for the examination of nonlinear refraction of laser radiation with vertical (*a*) and horizontal (*b*) sample positioning.

Total refraction index n for the medium exhibiting nonlinear optical effects is determined as

$$n = n_{lin} + n_{nlin} I, \tag{3}$$

where n_{lin} is the linear refraction index, n_{nlin} is the nonlinear refraction index, and I is the intensity of radiation incident on the sample. When laser radiation acts on a dispersed medium with a nonlinear refraction index, a phase non-uniformity arises in it, which induces a phase shift of radiation emerging from the sample. Nonlinear phase change $\varphi(r)$ as a function of distance from the beam center in an elementary layer of a nonlinear optical medium with thickness dz is written as

$$\varphi(r) = \frac{2\pi}{\lambda}\left(\int n dz - \int n_{lin} dz\right), \tag{4}$$

where λ is the wavelength. Nonlinear refraction index n_{nlin} may be determined using the Fresnel–Kirchhoff diffraction integral with the imposed conditions of a Gaussian spatial profile of the beam incident on the sample, a short optical path in the sample, and near-field positioning of the screen:

$$I(r') = \frac{1}{\lambda} I_0 \int_0^{\infty} \exp\left(-\frac{2r^2}{w_0^2}\right) \exp\left[i\left(-k\frac{(r-r')^2}{2R}\right)\right.$$
$$\left. + n_{nlin} I_0 d \exp\left(-\frac{2r^2}{w_0^2}\right)\right] dr, \tag{5}$$

where R is the radius of curvature of the wave front.

2. Results and Discussion

2.1. Characterization of the used SWCNTs and dispersed media based on them

Films on a silicon substrate were formed for Raman studies by spray deposition from the prepared liquid dispersed media (Fig. 4, *a*). The shape of the obtained Raman spectrum is typical of single-wall semiconductor carbon nanotubes. The RBM mode is represented as a broad band with a maximum at $185\,\mathrm{cm}^{-1}$ and a shoulder around 152, 162, and $176\,\mathrm{cm}^{-1}$. This is indicative of the presence of SWCNTs with different chirality; the modes from each SWCNT type overlap with one another, forming a single broad mode. The splitting of mode G into high-intensity G^+ ($1591\,\mathrm{cm}^{-1}$) and low-intensity G^- ($1570\,\mathrm{cm}^{-1}$) peaks suggests that carbon nanotubes are semiconducting in nature. The intensity ratio between modes G and D is a parameter often used to evaluate the amount of localized defects that may affect electron transport when a nanotube passes to an excited state. The I_D/I_G ratio for the SWCNT film was 0.038, which is indicative of a low density of defects in the initial carbon nanotubes. Mode D (with a maximum at $1344\,\mathrm{cm}^{-1}$) is represented by a broadened band, which is probably attributable to the influence of structural order defects of various kinds that include the presence of pentagons or heptagons in the nanotube plane, amorphous carbon, etc. SEM images (Fig. 4, *b*) reveal individual bundles of SWCNTs with a diameter of ~ 15 nm. The length of carbon nanotubes varies and may reach $\sim 5\,\mu$m.

The plot of the wavelength dependence of linear transmittance for the liquid dispersed medium with SWCNTs in DMF (Fig. 4, *c*) features a region of enhanced absorption near 300 nm; however, at a wavelength of 350 nm, the linear transmittance is already at the level of $\sim 65\,\%$, which is acceptable for photonic applications. A small plateau typical of SWCNTs is seen in the 650–750 nm spectral region. In the visible and near IR ranges, the linear transmittance spectrum is a uniform monotonic curve with a transmittance level above 70 %. The obtained spectra do not contain any pronounced absorption bands typical of individual nanotubes [24], indicating the presence of unsorted bundles of nanotubes, which are characterized by blurring of the characteristic individual absorption bands of SWCNTs [25,26]. The aqueous medium with SWCNTs behaved in a similar fashion in the visible and near IR spectral regions; the only difference is the absorption peak near 970 nm, which is identified as the absorption peak of water.

According to the results of DLS studies performed 24 h after the preparation of the samples, a significant contribution to light scattering (about 25 %) in the aqueous-based dispersed medium is produced by large agglomerates (larger than $5\,\mu$m). This is indicative of an increased concentration of such particles and, consequently, lower dispersion stability. Moving in the medium under the influence of Brownian or thermal motion, individual particles twist together and may subsequently precipitate, reducing the true concentration of nanoparticles. In the DMF-based medium, the primary contribution to scattering (above 90 %) is produced by individual bundles of SWCNTs with a hydrodynamic radius on the order of 250 nm. This is attributable to the lower (compared to water) surface tension of DMF, which facilitates the dispersion of SWCNTs.

2.2. Nonlinear limiting in dispersed media with SWCNTs and possible applications

Characteristic dependences plotted based on the results of *Z*-scanning and the experiment with a fixed sample position are presented in Fig. 5. In the aqueous-based dispersed medium with SWCNTs (Fig. 5, *a*), the normalized transmittance starts decreasing when the sample reaches the ≈ -15 mm mark on optical axis *Z*. As the focus of the lens is approached, the normalized transmittance decreases further, reaching ≈ 0.15 at point $z = 0$ corresponding to the focus. After that, the normalized transmittance increases gradually toward the initial level, which indicates that the dispersed medium has restored its linear transmittance. The plot of the dependence of transmitted laser energy fluence on the laser energy fluence incident on the sample (Fig. 5, *b*) features slight energy fluctuations, which may be attributed

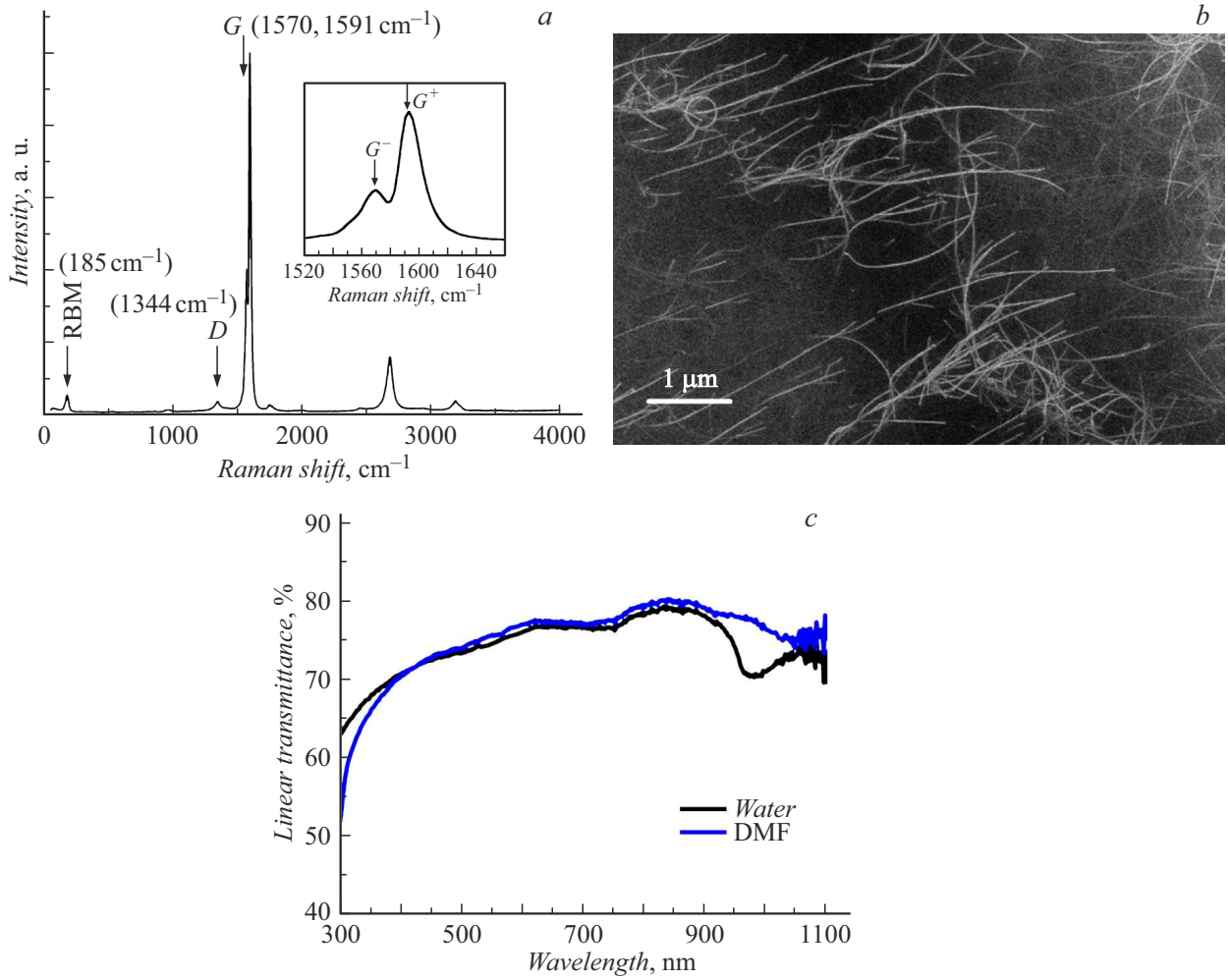

Figure 4. Raman spectrum (a) and SEM images (b) of the used SWCNTs and optical transmittance spectra of dispersed media with SWCNTs in different solvents (c).

Values of nonlinear optical parameters of the studied dispersed media

Material	Linear transmittance, %	Linear absorption coefficient, cm^{-1}	Effective nonlinear absorption coefficient, cm/GW	Threshold laser energy fluence, J/cm^2
SWCNTs in water	74	1.5	78	0.2
SWCNTs in DMF	73	1.57	135	0.17

to the presence of large agglomerates in the medium and the scattering of radiation by them.

The dispersed medium with SWCNTs in DMF exhibits a stronger nonlinear optical response, which is evidenced by a more profound reduction of the normalized transmittance at the lens focus (to a level of 0.09; see Fig. 5, c). It is also worth noting that the transmittance value starts to deviate from the linear one earlier, when the sample is positioned on the optical axis at ≈ -23 mm. This suggests that the laser energy fluence is lower compared to the aqueous dispersed medium. The plot of the dependence of transmitted laser energy fluence on the incident one has no visible outliers, which is indicative of high stability of the dispersed medium based on SWCNTs in DMF. The limiting curve (Fig. 5, d) is sharper in nature than the one for the aqueous dispersed medium.

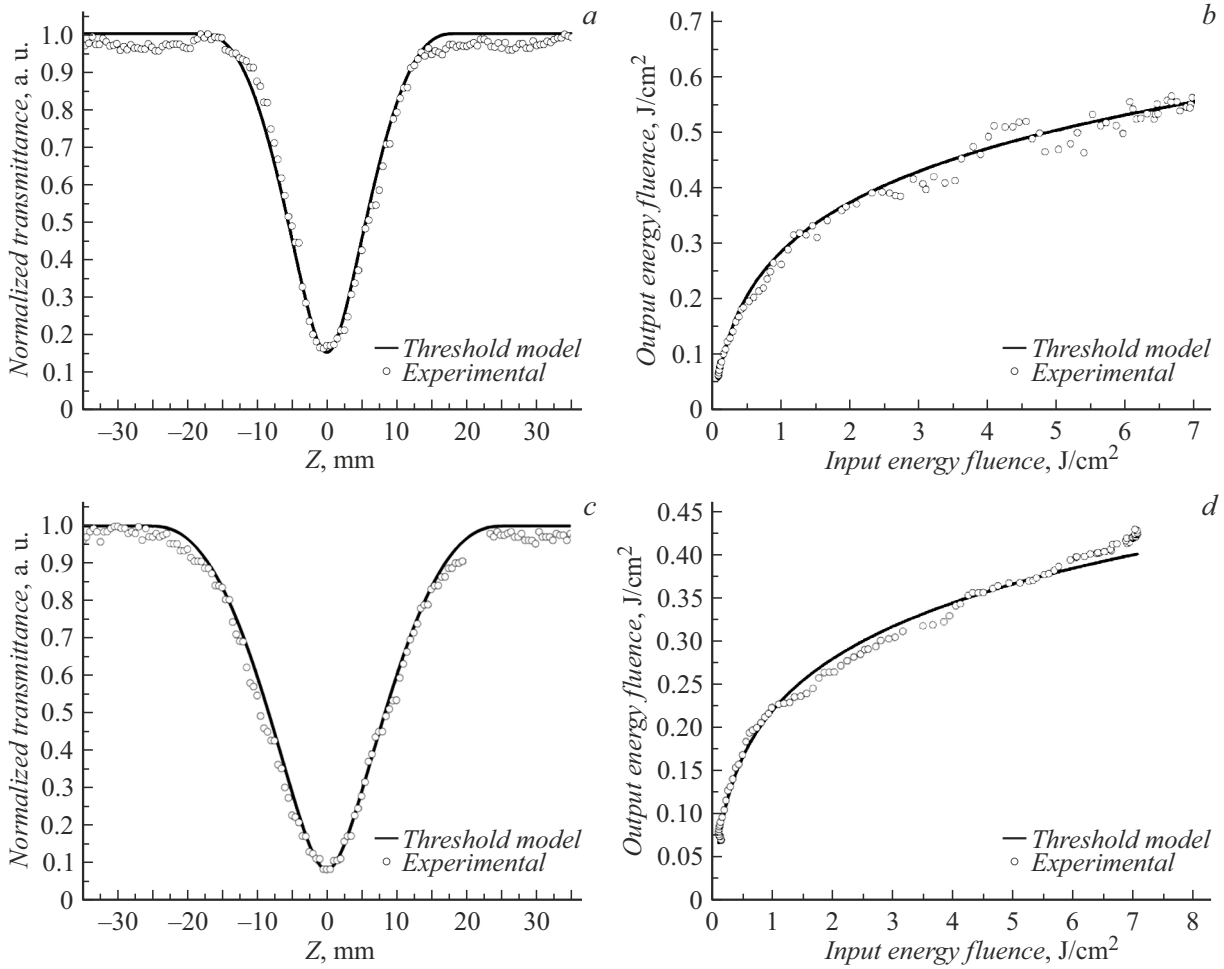

Figure 5. Plots of the dependence of normalized transmittance on the position of the nanodispersed medium relative to the lens focus (a, c) and the dependence of laser energy fluence transmitted through the medium on the incident laser energy fluence (b, d).

The obtained dependences were used to determine the values of the linear absorption coefficient, the effective nonlinear absorption coefficient, and the threshold laser energy fluence for the studied dispersed media. The calculation results are presented in the table.

In addition to recording the change in normalized transmittance during Z-scanning, the dependence of width of the laser pulse transmitted through the nanodispersed medium based on SWCNTs on the position of the nanodispersed medium was examined in the Z-scanning experiment (Fig. 6). Away from the focus, where the transmittance of dispersed media does not change, the width of the laser pulse transmitted through the medium also remains unchanged and equal to that of the pulse incident on the medium. When the normalized transmittance drops below 0.8, the transmitted pulse width starts to decrease, reaching ≈ 12 ns for the aqueous dispersed medium with SWCNTs and ≈ 10 ns for SWCNTs in DMF at the lens focus.

This change in pulse width is due to nonlinear optical effects in the dispersed medium. In the case of linear interaction, the shape of the leading and trailing edges of a laser pulse does not change. With nonlinear limiting and a reduction in normalized transmittance, the leading edge is also transmitted without changes (as can be seen in Fig. 6, b at $Z = 0$), while the trailing edge undergoes a nonlinear interaction and becomes steeper than in the linear case. However, the nature of nonlinear optical processes is still under debate. Inverse saturable absorption [27], multiphoton processes [28], and the effects of nonlinear scattering by thermally induced inhomogeneities (microplasma or solvent bubbles) [29] are noted among the nonlinear optical effects leading to limiting of nanosecond laser pulses in media with SWCNTs. It is known that optical limiting in carbon nanotube suspensions is induced primarily by nonlinear scattering by inhomogeneities formed due to absorption-induced heating, while limiting in a solubilized-type dispersed medium is caused by nonlinear absorption [30]. In most cases, nonlinear limiting is the result of not just a single nonlinear optical effect, but of a combination of several processes, which produces a synergistic effect [31]. Specifically, scattering may extend the optical path of photons inside the sample, which also leads to an increase in absorption [32].

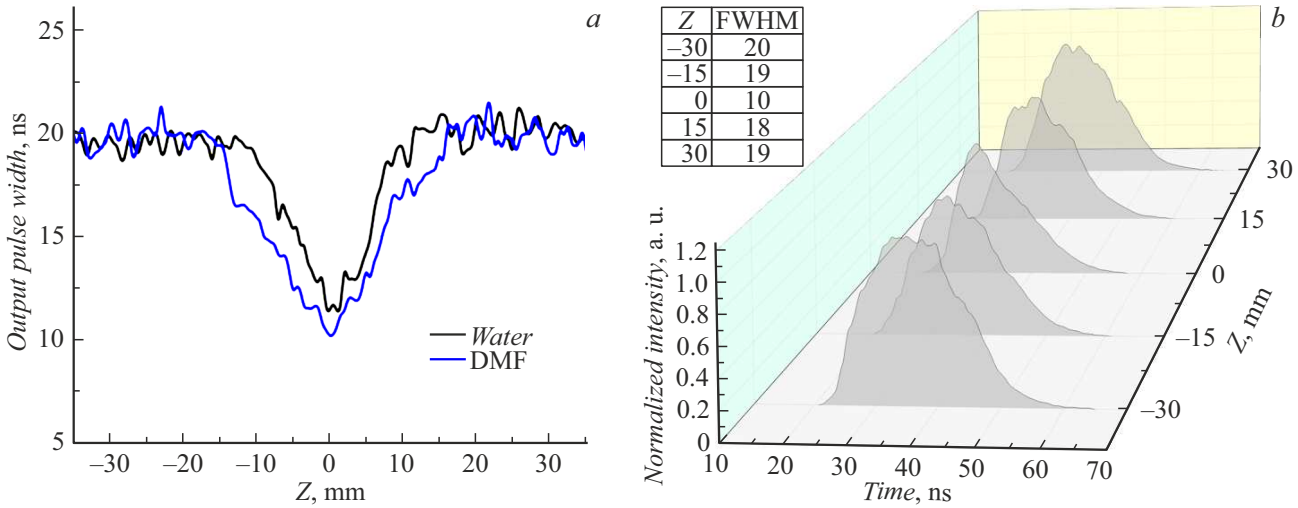

Figure 6. Plots of the dependences of transmitted laser pulse width (a) and time profiles of the beam (b) on the position of the sample relative to the lens focus.

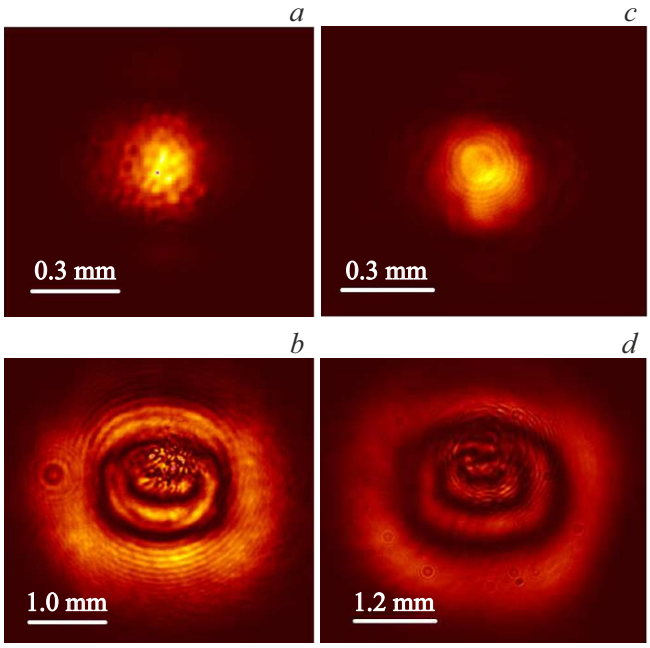

Figure 7. Interference patterns recorded with the incidence of quasi-continuous radiation on nanodispersed media based on SWCNTs in water (a, b) and DMF (c, d) in the case of vertical sample positioning: a — $P = 10$ mW, $D_x = 290\,\mu$m, $D_y = 290\,\mu$m; b — $P = 300$ mW, $D_x = 3000\,\mu$m, $D_y = 2600\,\mu$m; c — $P = 10$ mW, $D_x = 290\,\mu$m, $D_y = 290\,\mu$m; d — $P = 300$ mW, $D_x = 3500\,\mu$m, $D_y = 3100\,\mu$m.

The possibility of nonlinear limiting of individual nanosecond laser pulses makes dispersed media with SWCNTs promising materials for use as laser radiation limiters protecting photosensitive arrays in optical devices. A linear transmittance above 70 % allows one to achieve a high level of „useful“ signal. The presence of SWCNT bundles in a dispersed medium ensures a monotonic nature of the optical transmittance spectrum and the lack of color distortion, which is also important for optical limiters designed to protect the organs of vision. We proposed the design of a limiter with its key element being a nonlinear optical medium based on SWCNTs. A confocal lens system with a focal length of 4 cm was proposed as a means to enhance the nonlinear optical response. The confocal arrangement of lenses also helps avoid spatial shape alterations. The liquid dispersed medium with SWCNTs is introduced into a special cell with calcium fluoride glasses. The optical path length in the cell is adjusted with the use of special inserts.

2.3. Nonlinear refraction in dispersed media with SWCNTs and possible applications

The features of nonlinear refraction in dispersed media with SWCNTs were studied using a femtosecond laser at a pulse repetition rate of 80 MHz. Spatial beam profiles were determined at different radiation powers incident on the sample (Fig. 7). The beam diameters along the X and Y axes (D_x and D_y, respectively) were determined at the $1/e^2$ level. When diffraction rings were formed, the beam size was calculated as the radius of the outer ring. To avoid overexposure of the spatial beam analyzer array, different exposure values were set for different powers. At a low average radiation power (~ 10 mW), the transmitted beam has a Gaussian shape with a size similar to the beam size in the experiment without a sample. The laser beam starts to broaden noticeably at radiation power $P \approx 100$ mW. In addition, the increase in power leads to the formation of a ring-shaped beam structure. The beam broadening observed in the dispersed medium with SWCNTs in DMF was greater than that in the aqueous medium.

The emergence of such an interference pattern is the result of spatial self-phase modulation [33]. Refraction index n in the dispersed medium with SWCNTs changes under the

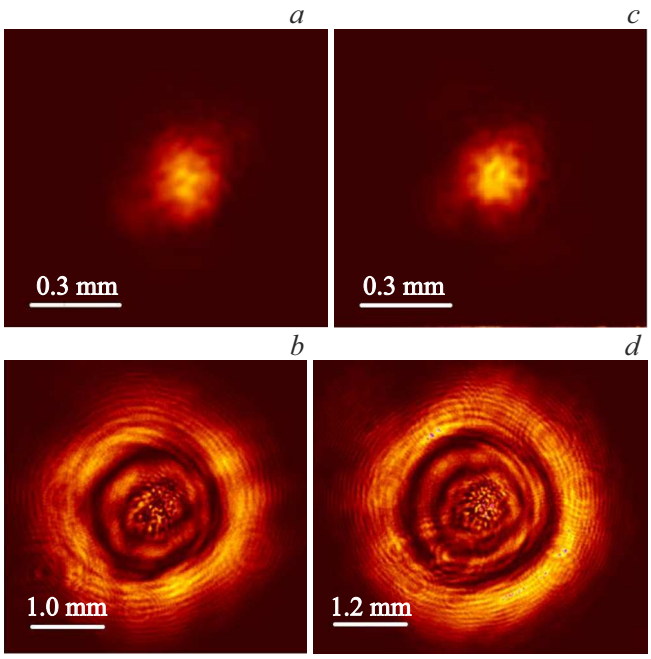

Figure 8. Interference patterns recorded with the incidence of quasi-continuous radiation on nanodispersed media based on SWCNTs in water (a, b) and DMF (c, d) in the case of horizontal sample positioning: a — $P = 10$ mW, $D_x = 290\,\mu$m, $D_y = 290\,\mu$m; b — $P = 300$ mW, $D_x = 3200\,\mu$m, $D_y = 3150\,\mu$m; c — $P = 10$ mW, $D_x = 290\,\mu$m, $D_y = 300\,\mu$m; d — $P = 300$ mW, $D_x = 3600\,\mu$m, $D_y = 3600\,\mu$m.

influence of laser radiation in accordance with formula (3). Since the incident laser beam has a Gaussian shape, the refraction index at the center of the irradiation site changes more profoundly than at the edges, inducing a refraction index gradient and, consequently, self-defocusing of the beam (i.e., its broadening).

The refraction index also affects the velocity of propagation of radiation in the medium. In view of the gradient refraction index variation, different parts of the beam propagate through the dispersed medium with SWCNTs at different velocities, which leads to a phase difference on emergence from the sample. Owing to this, a pattern in the form of rings, where light and dark rings correspond to the interference maxima and minima, forms on the screen (the photosensitive array of the spatial beam profile analyzer).

When the sample is positioned vertically, the interference pattern is, in contrast to the horizontal sample positioning, asymmetric: the radius of rings in the upper part of the beam decreases (Fig. 8). This shift is indicative of asymmetry of the phase non-uniformity in the dispersed medium, which may be attributed to the emergence of convective heat flows [34].

In the case of vertical positioning of the cell with the dispersed medium, heat flows are directed perpendicular to the axis of propagation of the laser beam, which leads to distortion of the interference pattern. With the horizontal arrangement, heat flows are collinear to the laser beam, and convection does not affect the shape of the phase non-uniformity and, as a consequence, the interference pattern.

The spatial self-phase modulation of a dispersed medium with SWCNTs may be used as one of the mechanisms of nonlinear power attenuation in laser radiation limiters. To illustrate the limiting properties of dispersed media with SWCNTs, we measured the dependences of radiation power transmitted through the sample on the incident radiation power (with the cell positioned horizontally; see Fig. 9).

A region of linear interaction, where the entire laser beam remains within the bounds of the detector, is seen at a power below 100 mW. However, when the beam broadens beyond the detector diameter, a power limiting effect emerges. The obtained dependences are similar in shape to the one corresponding to an ideal limiter. The plotted curve is wavy due to the light and dark rings falling on the edge of the detection region. In addition, this dependence was used to determine nonlinear refraction index n_{nlin} of dispersed media with SWCNTs; in this case, boundary conditions corresponding to the diameter of the open part of the detector were added to formula (5). The nonlinear refraction index was determined by the least squares method (i.e., by finding the minimum of the sum of deviations of the approximating function values (solid curve in the plots) from the experimental values (dots)). The following magnitudes of the nonlinear refraction index were obtained for the dispersed media with SWCNTs in water and DMF: (0.18 ± 0.01) cm^2/MW and (0.28 ± 0.01) cm^2/MW. Such differences are indicative of a strong influence of the solvent properties on nonlinear refraction. This is attributable to the lower thermal conductivity coefficient of DMF (0.19 W/(m·K) versus 0.61 W/(m·K) for water), which translates into a steeper refraction index gradient, and also indicates that nonlinear refraction in these media is thermal in nature.

In addition, the feasibility of application of dispersed media with SWCNTs as nonlinear optical switches for signal transmission in optical communication systems was investigated. The aperture in front of the power sensor was repositioned in these experiments in such a way that a low-power beam could not pass through the open part of the aperture, but radiation started to reach the sensor when the beam expanded and interference rings appeared. The open part of the aperture is represented by the green circle in Fig. 10. The results of this experiment were processed to obtain a dependence that characterizes the occurrence of interference maxima and minima (light and dark rings) in the detector region. Taking the interference maximum as a logical „one“ and the interference minimum as a logical „zero,“ one may implement fully optical signal transmission by varying the power of laser radiation.

Conclusion

Liquid dispersed media with SWCNTs may exhibit various nonlinear optical properties depending on the nature of

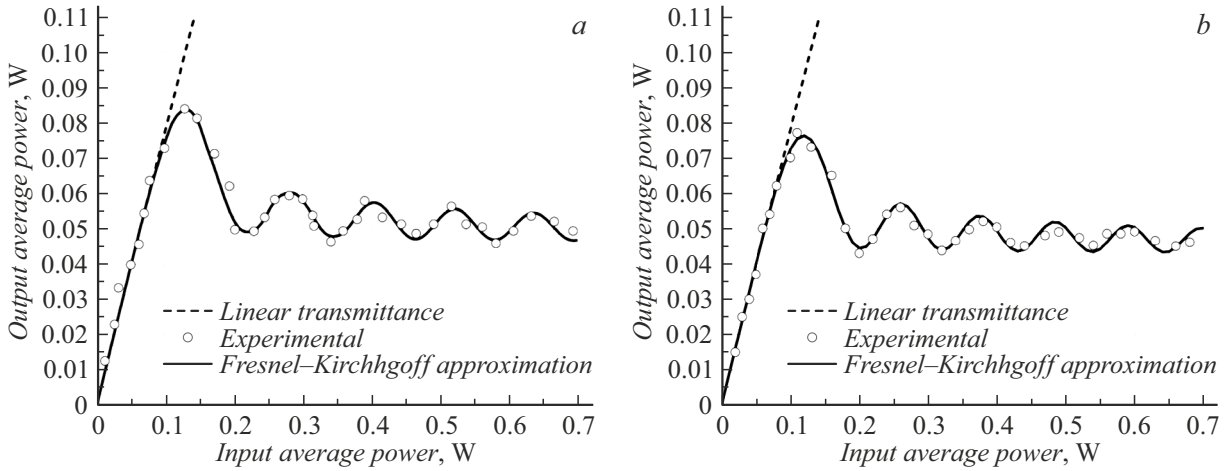

Figure 9. Dependence of transmitted power on the power of incident radiation for the nanodispersed medium of SWCNTs in water (*a*) and in DMF (*b*).

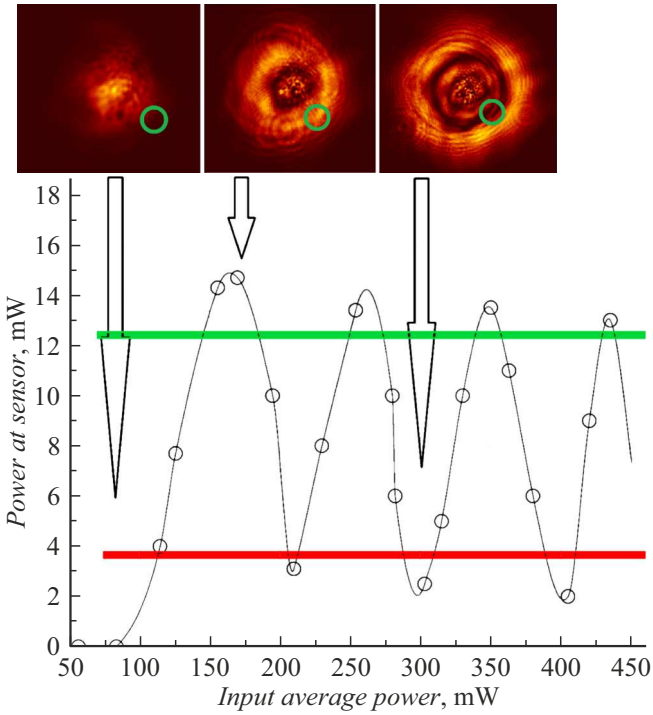

Figure 10. Transmission of logical „zeros“ and „ones“ depending on the power of radiation incident on the dispersed medium.

laser exposure. Experimental setups based on nanosecond and femtosecond lasers allow one to study nonlinear limiting and nonlinear refraction of light, respectively.

A suppression of normalized transmittance of dispersed media exposed to individual nanosecond pulses, which is also accompanied by a change in the laser pulse width, was demonstrated. The high speed of nonlinear optical response makes such materials suitable for ultrafast laser signal limiting and control. Irradiation with ultrashort pulses with a high repetition rate induces a change in the refraction index of dispersed media with SWCNTs. Nonlinear refraction of light leads to the modulation of spatial shape of the beam (its broadening) and the formation of interference rings. The effect of convection flows emerging under the influence of laser radiation on the symmetry of the interference pattern was revealed. The enhanced nonlinear optical response in DMF media is attributable to the fact that this solvent has a lower thermal conductivity than water, which leads to the formation of a steeper refraction index gradient at the irradiation site. The applicability of nonlinear refraction of light in dispersed media with SWCNTs in nonlinear limiting of radiation with a high pulse repetition rate and in switching of logical states by optical signal control was demonstrated.

Funding

This study was performed as part of a major research project and supported financially by the Ministry of Science and Higher Education of the Russian Federation under agreement No. 075-15-2024-555 dated April 25, 2024.

Conflict of interest

The authors declare that they have no conflict of interest.

References

[1] Y.C. Shin, B. Wu, S. Lei, G.J. Cheng, Y. Lawrence. Int. J. Manuf. Eng., **142** (11), 110818 (2020). DOI: 10.1115/1.4048397
[2] R.M. Ma, R.F. Oulton. Nat. Nanotechnol., **14** (1), 12 (2019). DOI: 10.1038/s41565-018-0320-y
[3] X. Wang, Y. Cui, T. Li, M. Lei, J. Li, Z. Wei. Adv. Opt. Mater., **7** (3), 1801274 (2019). DOI: 10.1002/adom.201801274
[4] N. Li, C.P. Ho, J. Xue, L.W. Lim, G. Chen, Y.H. Fu, L.Y.T. Lee. Laser Photon. Rev., **16** (11), 2100511 (2022). DOI: 10.1002/lpor.202100511

[5] P. Dong, Y.K. Chen, G.H. Duan, D.T. Neilson. Nanophotonics, **3** (4-5), 215 (2014). DOI: 10.1515/nanoph-2013-0023
[6] P. Trocha, D. Ganin, M. Karpov, M.H.P. Pfeiffer, A. Kordts, J. Krockenberger, S. Wolf, P. Marin-Palomo, C. Weimann, S. Randel, W. Freude, T.J. Kippenberg, C. Koos. Science, **359** (6378), 887 (2018). DOI: 10.1126/science.aao3924
[7] G.H. Lee, H. Moon, H. Kim, G.H. Lee, W. Kwon, S. Yoo, D. Myung, S.H. Yun, Z. Bao, S.K. Hahn. Nat. Rev. Mater., **5** (2), 149 (2020). DOI: 10.1038/s41578-019-0167-3
[8] J. Wu, J. Peng, B. Liu, T. Pan, H. Zhou, J. Mao, Y. Yang, C. Qiu, Y. Su. Opt. Commun., **373**, 44 (2016). DOI: 10.1016/j.optcom.2015.07.045
[9] L. Wu, Y. Dong, J. Zhao, D. Ma, W. Huang, Y. Zhang, Y. Wang, X. Jiang, Y. Xiang, J. Li, Y. Feng, J. Xu, H. Zhang. Adv. Mater., **31** (14), 1807981 (2019). DOI: 10.1002/adma.201807981
[10] D. Dai. Proc. IEEE, **106** (12), 2117 (2018). DOI: 10.1109/JPROC.2018.2822787
[11] S. Fathpour. IEEE J. Quant. Electron., **54** (6), 1 (2018). DOI: 10.1109/JQE.2018.2876903
[12] T.C. Wei, S. Mokkapati, T.Y. Li, C.H. Lin, G.R. Lin, C. Jagadish, J.H. He. Adv. Funct. Mater., **28** (18), 1707175 (2018). DOI: 10.1002/adfm.201707175
[13] D. Dini, M.J.F. Calvete, M. Hanack. Chem. Rev., **116** (22), 13043 (2016). DOI: 10.1021/acs.chemrev.6b00033
[14] P. Kabaciński, T.M. Kardaś, Y. Stepanenko, C. Radzewicz. Opt. Express, **27** (8), 11018 (2019). DOI: 10.1364/OE.27.011018
[15] P. Khan, R.K. Yadav, A. Mondal, C.S. Rout, K.V. Adarsh. Opt. Mater., **120**, 111459 (2021). DOI: 10.1016/j.optmat.2021.111459
[16] S. Pascal, S. David, C. Andraud, O. Maury. Chem. Soc. Rev., **50** (11), 6613 (2021). DOI: 10.1039/D0CS01221A
[17] M.S. Savelyev, P.N. Vasilevsky, Yu.P. Shaman, A.Yu. Tolbin, A.Yu. Gerasimenko, S.V. Selishchev. Tech. Phys., **68** (4), 476 (2023). DOI: 10.21883/TP.2023.04.55939.281-22
[18] L. Wu, X. Jiang, J. Zhao, W. Liang, Z. Li, W. Huang, Z. Lin, Y. Wang, F. Zhang, S. Lu, Y. Xiang, S. Xu, J. Li, H. Zhang. Laser Photon. Rev., **12** (12), 1800215 (2018). DOI: 10.1002/lpor.201800215
[19] J. Wang, Y. Chen, W.J. Blau. J. Mater. Chem., **19** (40), 7425 (2009). DOI: 10.1039/B906294G
[20] P.N. Vasilevsky, M.S. Savelyev, A.Yu. Tolbin, A.V. Kuksin, Y.O. Vasilevskaya, A.P. Orlov, Y.P. Shaman, A.A. Dudin, A.A. Pavlov, A.Yu. Gerasimenko. Photonics, **10** (5), 537 (2023). DOI: 10.3390/photonics10050537
[21] W.B. Cho, J.H. Yim, S.Y. Choi, S. Lee, A. Schmidt, G. Steinmeyer, U. Griebner, V. Petrov, D.-I. Yeom, K. Kim, F. Rotermund. Adv. Funct. Mater., **20** (12), 1937 (2010). DOI: 10.1002/adfm.200902368
[22] S. Berciaud, L. Cognet, P. Poulin, R.B. Weisman, B. Lounis. Nano Lett., **7** (5), 1203 (2007). DOI: 10.1021/nl062933k
[23] S.A. Tereshchenko, M.S. Savelyev, V.M. Podgaetsky, A.Yu. Gerasimenko, S.V. Selishchev. J. Appl. Phys., **120** (9), 093109 (2016). DOI: 10.1063/1.4962199
[24] M.J. O'Connell, S.M. Bachilo, C.B. Huffman, V.C. Moore, M.S. Strano, E.H. Haroz, K.L. Rialon, P.J. Boul, W.H. Noon, C. Kittrell, J. Ma, R.H. Hauge, R.B. Weisman, R.E. Smalley. Science, **297** (5581), 593 (2002). DOI: 10.1126/science.1072631
[25] A.G. Ryabenko, T.V. Dorofeeva, G.I. Zvereva. Carbon, **42**, 1523 (2004). DOI: 10.1016/j.carbon.2004.02.005
[26] S.D. Shandakov, M.V. Lomakin, A.G. Nasibulin. Tech. Phys. Lett., **42** (11), 1071 (2016). DOI: 10.1134/S1063785016110080
[27] B. Anand, S.A. Ntim, V.S. Muthukumar, S.S.S. Sai, R. Philip, S. Mitra. Carbon, **49** (14), 4767 (2011). DOI: 10.1016/j.carbon.2011.06.086
[28] J. Shi, H. Chu, Y. Li, X. Zhang, H. Pan, D. Li. Nanoscale, **11** (15), 7287 (2019). DOI: 10.1039/C8NR10174D
[29] Y. Chen, Y. Lin, Y. Liu, J. Doyle, N. He, X. Zhuang, J. Bai, W.J. Blau. J. Nanosci. Nanotechnol., **7** (4-5), 1268 (2007). DOI: 10.1166/jnn.2007.308
[30] S. Rahman, S. Mirza, A. Sarkar, G.W. Rayfield. J. Nanosci. Nanotechnol., **10** (8), 4805 (2010). DOI: 10.1166/jnn.2010.2746
[31] K. Mansour, M.J. Soileau, E.W. Van Stryland. JOSA B, **9** (7), 1100 (1992). DOI: 10.1364/JOSAB.9.001100
[32] M.S. Savelyev, A.Y. Gerasimenko, P.N. Vasilevsky, Y.O. Fedorova, T. Groth, G.N. Ten, D.V. Telyshev. Anal. Biochem., **598**, 113710 (2020). DOI: 10.1016/j.ab.2020.113710
[33] Y. Liao, C. Song, Y. Xiang, X. Dai. Ann. Phys., **532** (12), 2000322 (2020). DOI: 10.1002/andp.202000322
[34] Y. Shi, Y. Gao, Y. Hu, Y. Xue, G. Rui, L. Ye, B. Gu. Opt. Lasers Eng., **158**, 107168 (2022). DOI: 10.1016/j.optlaseng.2022.107168

Translated by D.Safin